Performance and feasibility of porous separators in Iron-Chromium flow batteries

J.P. du Toit, H.M. Krieg
North-West University, Potchefstroom, South Africa. Focus Area: Chemical Resource Beneficiation
[💻 henning.krieg@nwu.ac.za, ☎ +27-(0)18-299-1669, 🖷 +27-(0)18-299-1668]

Introduction

ICRFB

Favourable properties for upscaling[1]

- Capacity of flow batteries linked to electrolyte tank size
- Abundant electrolyte active materials Fe & Cr
  Low electrolyte cost: 17 USD kWh^{-1}
- SA: High annual solar irradiance (220 W m^{-2}) & low population density

Current challenges hindering commercialisation

- Lacking general development from insufficient research
- Capacity decay
- High cost of PFSA membrane: ≈ 500 USD m^{-2}

Research focus

Performance of commercially available porous separators

Celgard, Daramic & Entek

- Optimised for different technologies, e.g. LiB, VRFB…
- Fast acquisition without manufacturing
- Low cost
- Valuable insights on parameter optimisation

Wide range of properties

- Stretched, coated & extruded
- Thickness: 25 – 900 µm
- Permeability
- Symmetric & asymmetric
- PE, PP, PVDF, Phenolic resins & PTFE
- Hydrophilicity/ embedded Si

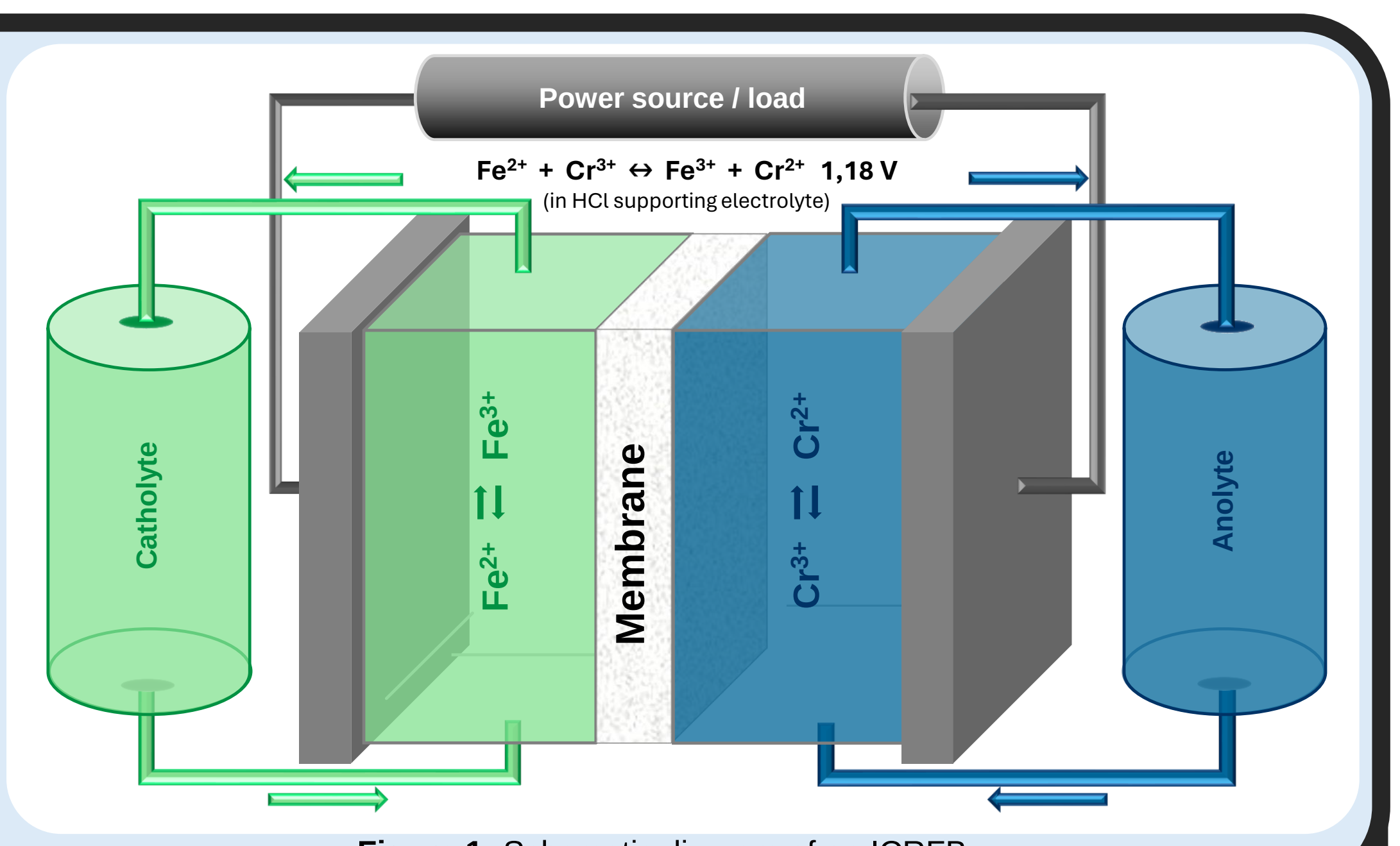

Figure 1: Schematic diagram of an ICRFB

Advantages

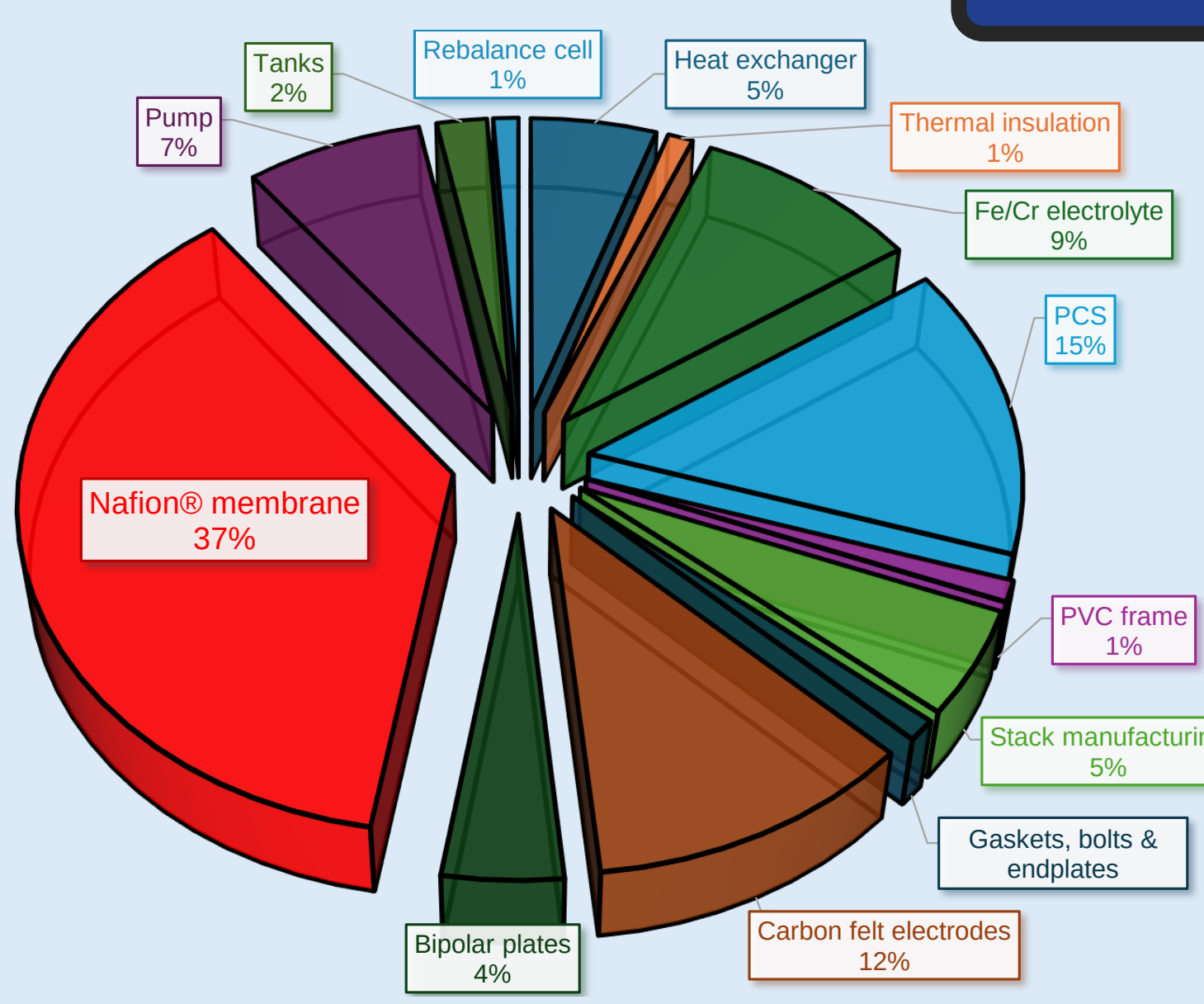

Figure 2: Cost breakdown of ICRFB @194 USD kWh^{-1}

PFSA to simple hydrocarbon separators[3]

	Nafion	MPS
Membrane cost (\$ m^{-2})	500	5
Membrane contribution to total cost (%)	37	0,6
Cost (\$ kWh^{-1})	194	123

ICRFB vs other flow batteries

- VRFB[2]
  - Lower oxidative environment than VRFB
    (V^{5+} 1.00 V vs Fe^{3+}: 0.771 V Cr^{3+}: – 0.408 V)
  - More non-fluorinated materials
  - Acidic stability, 1M HCl vs 3M H_2SO_4
- Aqueous system compared to organic RFBs
  - Majority of polymers vulnerable to solvents
- Fuel Cells
  - Materials susceptible to OH^- radical attacks

Experimental

Testing & characterisation

- Permeability
  GURLEY 4340 Automatic Densometer
- Chemical compatibility tests
- Discharge polarisation curves @ 0-180 mA cm^{-2}
- Charge/discharge @ 40,6 mA cm^{-2}
  Short term testing: 10-30 cycles
- Self-discharge tests
- SEM imaging

Conditions

- Electrolyte & cell @ 65,0 ± 0,2 °C
- Symmetric Fe/Cr electrolyte in 1M HCl
- Electrolyte pumping rate @ 20% above stoichiometric

Components

- AvCarb G650A graphite felt electrodes
  Thermally activated @ 650 °C for 30 min
- SGL Carbon 600 µm bipolar plates

1. Potentiostat
2. Heating plate
3. Nitrogen supply
4. Peristaltic pump
5. Water circulator
6. Temperature probe
7. RFB cell
8. Electrolyte heaters
9. Water circulating pipes

Figure 3: Lab-scale ICRFB test station

Results

Separator	Thickness (µm)	Density (g cm^{-3})	Gurley no. (s)	H_2O uptake (v/v%)	EE%	ASR (Ω cm²)	Hourly Cap Decay (%)
PP (A)	25	1.56	15099	38	25	4.35	8.55
PP (B)	38	2.00	586	0	X	X	X
PP (C)	75	2.75	1322	30	39	3.65	4.79
PE (A)	183	1.87	522	63	43	2.82	0.91
PE (B)	201	1.83	1135	39	57	2.39	2.74
Coated PE (B)	240	2.43	NP	32	X	X	X
PFSA on PTFE	243	1.60	NP	48	68	2.40	0.43
Phenol resin	456	2.30	111	69	X	X	X
PE (C)	884	2.22	3831	50	71	3.24	0.71
Nafion 212	51	---	NP	---	75	2.38	0.54

Performance vs properties

- CE% directly influenced by separation efficiency
- Low separation efficiency → Low EE%
- Separation efficiency more dependent on porous separator's **Thickness** than gas permeability
- Thickness ↑ ASR ↓ VE

Thickness of MPS most vital parameter

~200 µm MPS equivalent ASR to 51 µm CEM
~20 µm CEM coatings reduce convection

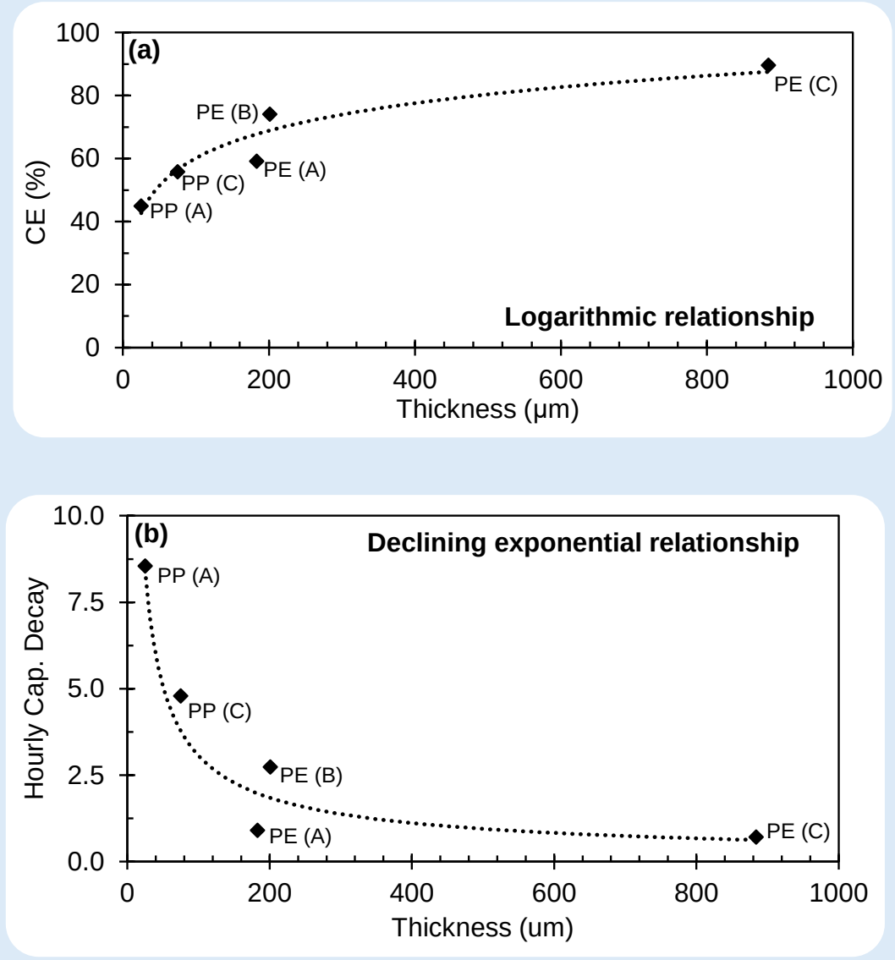

Figure 4: (a) Hourly capacity decay and (b) Coulombic efficiency, as functions of MPS thickness

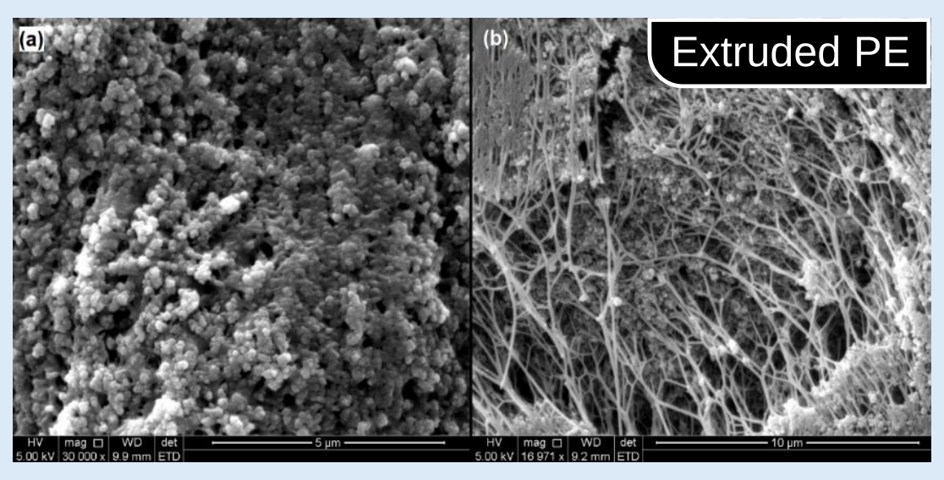

Figure 5: SEM imaging of MPS (a) Surface and (b) Cross section

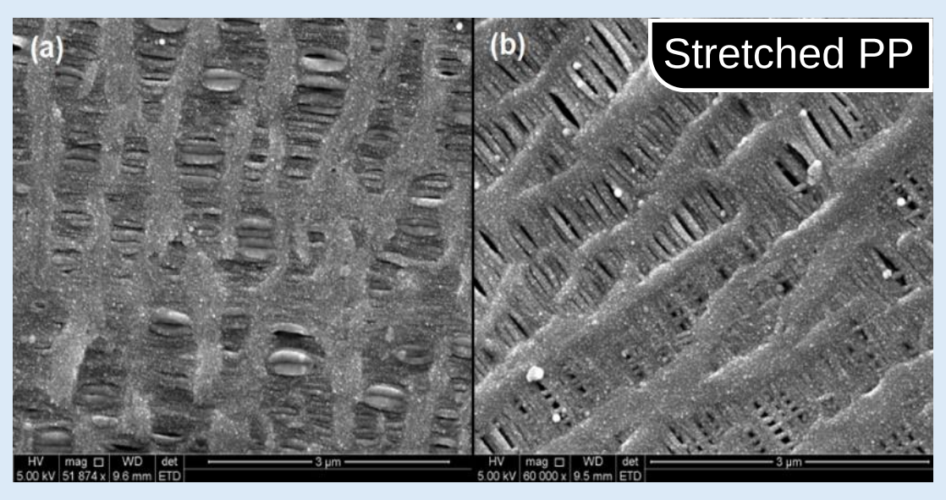

Figure 6: Surface SEM imaging of (a) Before and (b) After ICRFB cycling

Poor performance from convection crossover

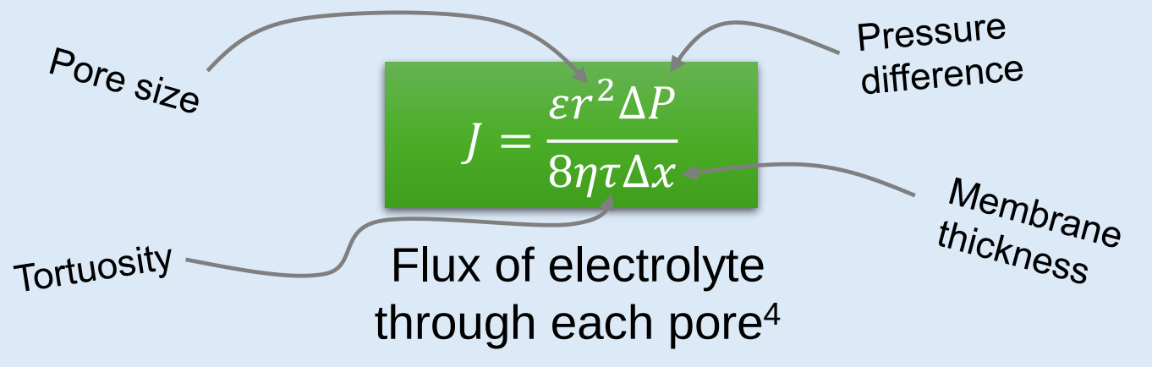

$$J = \frac{\varepsilon r^2 \Delta P}{8\eta\tau\Delta x}$$

Flux of electrolyte through each pore[4]

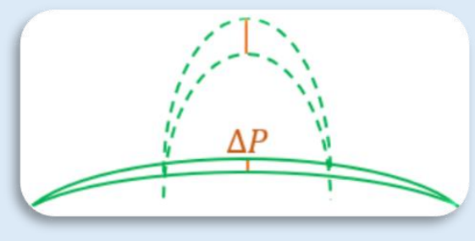

Pulsing from peristaltic pump

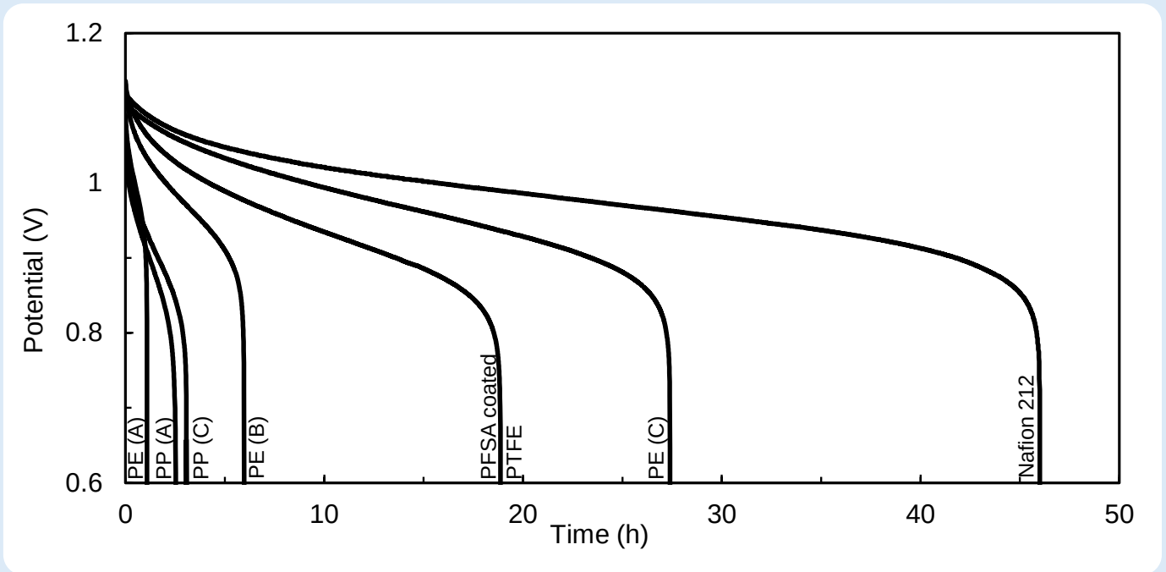

Figure 7: Self-discharge of various separators

Minimise ΔP across MPS

- Pulse dampening
- Hydraulic pressure balancing
- Asymmetric flowrate
  Anolyte/Catholyte viscosity variations with SOC

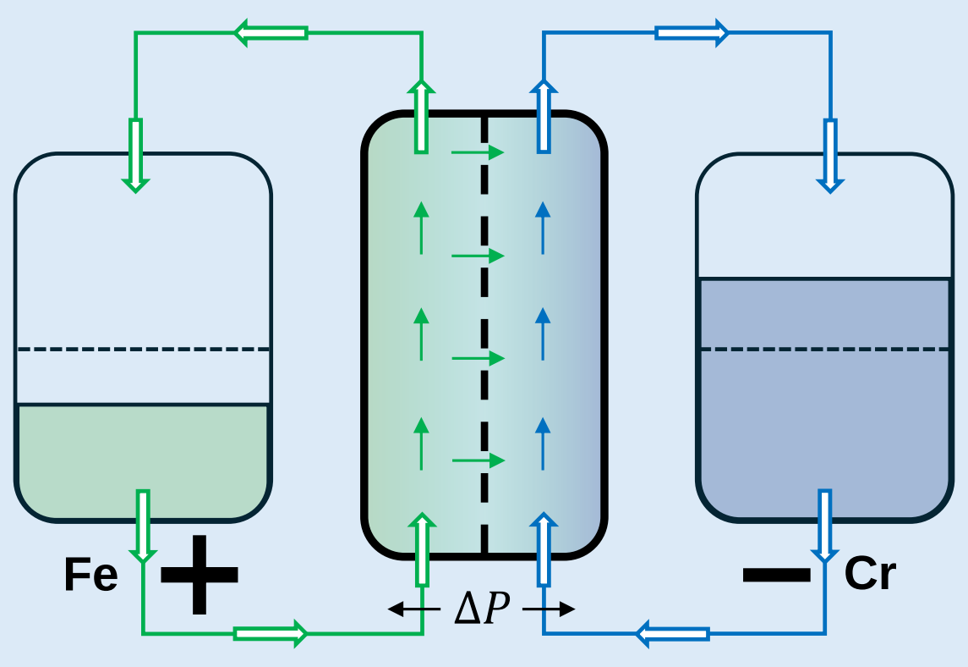

- Per cycle capacity decay down to 0.44%
- 5% increase in average EE
- 87.3% lower self-discharge rate
- 8.3% higher discharge capacity (Ah L^{-1})

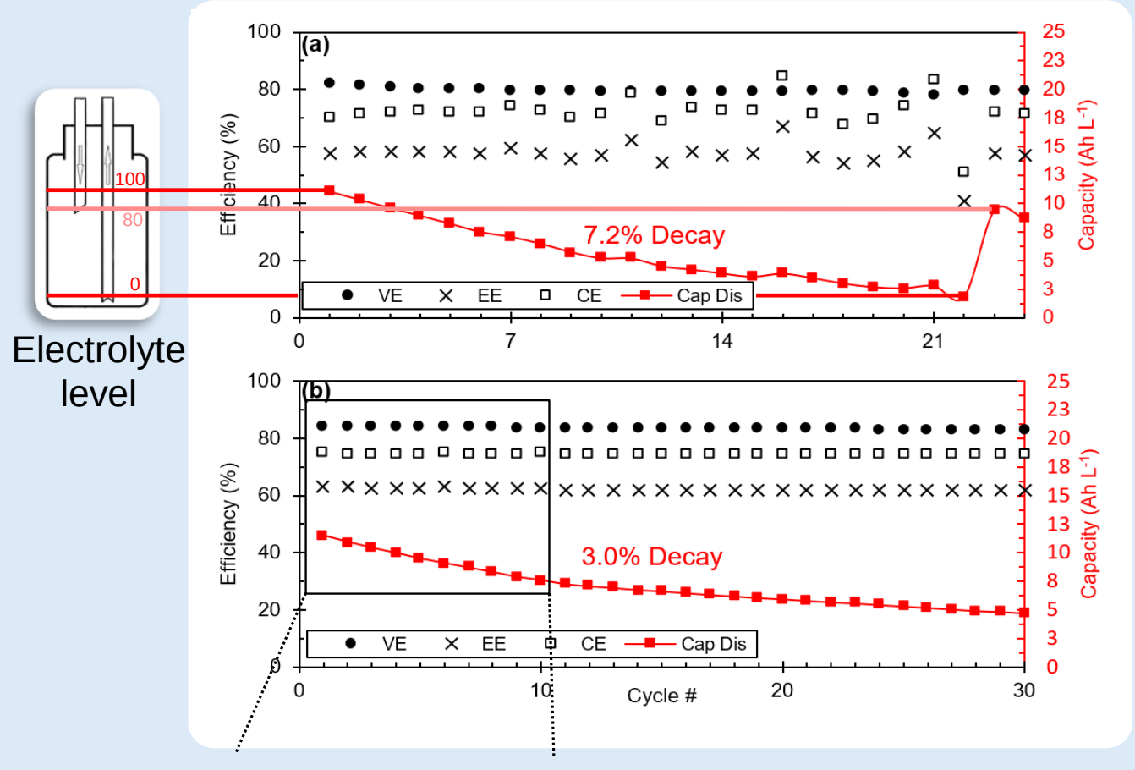

Figure 8: Performance over 30 cycles with **PE (B)** using (a) normal experimental setup and (b) fitted pulse dampener

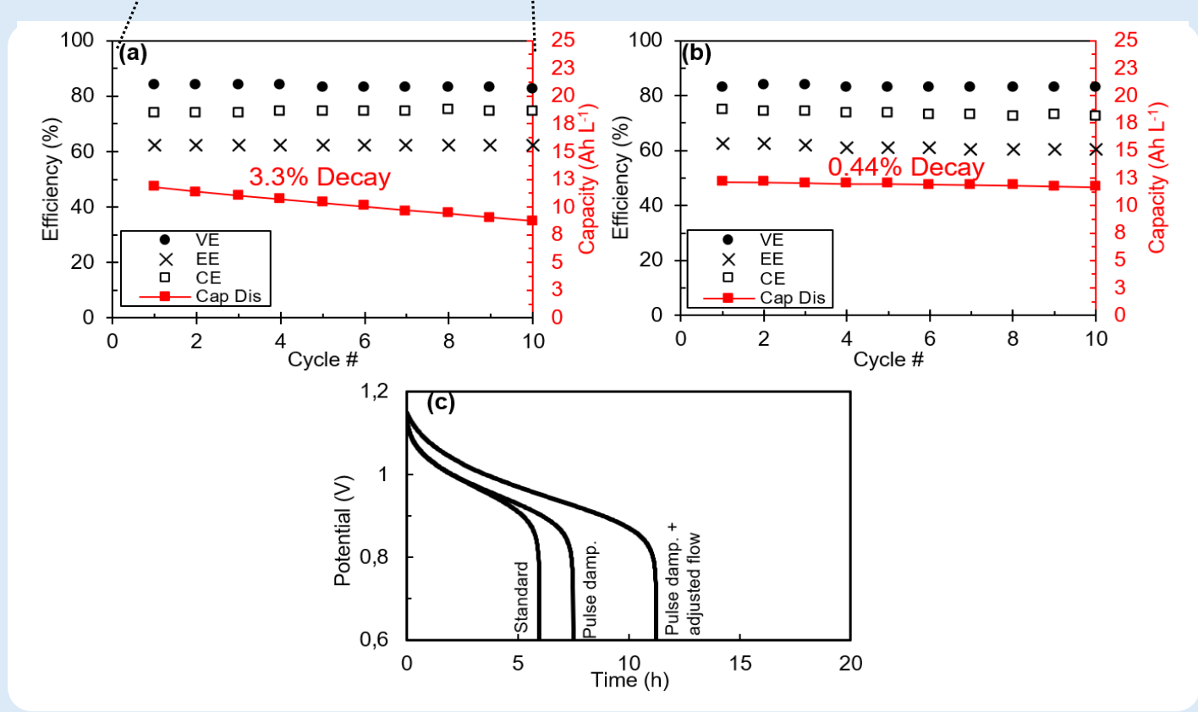

Figure 9: 10 cycle performance of **PE (B)** using (a) a pulse dampener and (b) a pulse dampener with increased anolyte flow**.** (c) Self-discharge curves of **PE (B)** comparing different pumping adaptations.

Conclusions

Performance vs PFSA benchmark

- 4.5% Lower EE
- Similar hourly capacity decay
- High chemical stability

Convection can be eliminated with basic, low-cost solutions

- Fitment of nitrogen filled tubing to act as pulse dampener
- Slight adjustment of flowrate
- Drastic decrease in capacity decay & self-discharge while increasing EE

Results support future feasibility of MPS technology in large-scale ICRFB systems

Challenges

- Convection crossover
- Specific parameter optimisation
  - Thickness
  - Membrane void space
  - Pore size
  - Porosity
  - Permeability
  - Wettability

Outlook

- Development of dynamic electrolyte pumping dependent on SOC
- Model development for ideal parameters through manufacturing of separators
- Synthesis and testing of low-cost ionomer coatings

References

1. Zeng, Y. K.; Zhao, T. S.; An, L.; Zhou, X. L.; Wei, L. A comparative study of all-vanadium and iron-chromium redox flow batteries for large-scale energy storage. *Journal of Power Sources* **2015**, *300*, 438-443.
2. Lu, W.; Yuan, Z.; Zhao, Y.; Zhang, H.; Zhang, H.; Li, X. Porous membranes in secondary battery technologies. *Chemical Society Reviews* **2017**, *46* (8),
3. Ha, S.; Gallagher, K. G. Estimating the system price of redox flow batteries for grid storage. *Journal of Power Sources* **2015**, *296*, 122-132.
4. Mulder, M. *Basic Principles of Membrane Technology*; Kluwer Academic Publishers, 1996.

NWU® | *Chemical Resource Beneficiation*